frontiers | Frontiers in Public Health

TYPE Original Research
PUBLISHED 01 February 2023
DOI 10.3389/fpubh.2022.1094771

OPEN ACCESS

EDITED BY
Niaz Muhammad Shahani,
China University of Mining and Technology, China

REVIEWED BY
Jian Zhou,
Central South University, China
Mohammadreza Koopialipoor,
Amirkabir University of Technology, Iran

*CORRESPONDENCE
Mahdi Hasanipanah
✉ hasanipanahmahdi@duytan.edu.vn

SPECIALTY SECTION
This article was submitted to Occupational Health and Safety, a section of the journal Frontiers in Public Health

RECEIVED 10 November 2022
ACCEPTED 29 November 2022
PUBLISHED 01 February 2023

CITATION
Keshtegar B, Piri J, Asnida Abdullah R, Hasanipanah M, Muayad Sabri Sabri M and Nguyen Le B (2023) Intelligent ground vibration prediction in surface mines using an efficient soft computing method based on field data. *Front. Public Health* 10:1094771. doi: 10.3389/fpubh.2022.1094771

Intelligent ground vibration prediction in surface mines using an efficient soft computing method based on field data

Behrooz Keshtegar[1], Jamshid Piri[2], Rini Asnida Abdullah[3], Mahdi Hasanipanah[3,4]*, Mohanad Muayad Sabri Sabri[5] and Binh Nguyen Le[4,6]

[1]Department of Civil Engineering, Faculty of Engineering, University of Zabol, Zabol, Iran, [2]Department of Water Engineering, Faculty of Water and Soil, University of Zabol, Zabol, Iran, [3]Department of Geotechnics and Transportation, Faculty of Civil Engineering, Universiti Teknologi Malaysia, Johor Bahru, Malaysia, [4]Institute of Research and Development, Duy Tan University, Da Nang, Vietnam, [5]Peter the Great St. Petersburg Polytechnic University, St. Petersburg, Russia, [6]School of Engineering and Technology, Duy Tan University, Da Nang, Vietnam

Ground vibration induced by blasting operations is considered one of the most common environmental effects of mining projects. A strong ground vibration can destroy buildings and structures, hence its prediction and minimization are of high importance. The aim of this study is to estimate the ground vibration through a hybrid soft computing (SC) method, called RSM-SVR, which comprises two main regression techniques: the response surface model (RSM) and support vector regression (SVR). The RSM-SVR model applies an RSM in the first calibrating process and an SVR in the second calibrating process to improve the accuracy of the ground vibration predictions. The predicted results of an RSM, which are obtained using the input data of problems, are used as the input dataset for the regression process of an SVR. The effectiveness and agreement of the RSM-SVR model were compared to those of an SVR optimized with the particle swarm optimization (PSO) and genetic algorithm (GA), RSM, and multivariate linear regression (MLR) based on several statistical factors. The findings confirmed that the RSM-SVR model was considerably superior to other models in terms of accuracy. The amounts of coefficient of determination (R^2) were 0.896, 0.807, 0.782, 0.752, 0.711, and 0.664 obtained from the RSM-SVR, PSO-SVR, GA-SVR, MLR, SVR, and RSM models, respectively.

KEYWORDS

blasting, ground vibration, hybrid soft computing method, RSM, SVR

1. Introduction

When excavating hard rock (which is required specifically in mining and quarrying operations, and generally when constructing highways, subways, tunnels, and dams), a common activity is drilling and blasting operations. As confirmed in the relevant literature, blasting unavoidably leads to some adverse impacts such as air blasts, ground vibrations, back breaks, flyrocks, and noise (Figure 1) (1–11). Although it is quite impossible to entirely eliminate all these impacts, they can be minimized. Ground vibration, among all, is one of the most important concerns in this sense (12–14). The extent of vibration occurred to a given structure is dependent upon different parameters such as the method of construction, distance from the source, soil/rock medium, heterogeneity of the soil and rock deposit, features of the waves propagated at the given site, the structure's susceptibility rating, the soil/rocks dynamic features, and the fracture's response characteristics (15, 16). Most of these parameters (particularly those related to geotechnical and geological conditions) are not controllable; however, the amount of explosive material and other blast design parameters such as burden (B), spacing (S), and powder factor (PF) can be controlled (17). The literature comprises different studies focusing on how to decrease the environmental impacts induced by blasting operations; though, due to the complexity of the problem, it lacks a general consistent approach or a certain formula in this regard. Not only the wave and ground motion features but also the complexity of blasting parameters and site factors has limited the scholars working in this field. This hinders the effective development of a widely-accepted criterion for measuring the geological parameters and blasting data and also ensuring the serviceability of susceptible constructions (18). It is possible to control the extent of ground vibration by choosing appropriate blasting methods and the best drilling/firing pattern. Generally, the vibration source produces body and surface waves in the rock/soil medium (16). Body waves are propagated through the rock and soil deposits. The most important types of body waves are compression and shear waves which need to be well considered at a comparatively small distance from the construction sources. On the other hand, the surface waves (whose main type is Rayleigh waves) are normally propagated along the upper surface of the ground. As building foundations are typically positioned near the ground surface, the Rayleigh waves usually attract great attention from structural engineers.

Peak particle velocity (PPV) and frequency are the most important descriptors in measuring blast-induced ground vibration. Among them, the former has been more widely used in previous studies (9–11). Accordingly, PPV is used in this study to measure ground vibration. The maximum charge used per delay (Mc) and distance from the blasting point (Di) (which have been used in various empirical approaches) are the two main parameters to calculate the PPV value. For example, Ghosh and Daemen (19), Gupta et al. (20, 21), and Roy (22) have presented several empirical approaches in this regard. In general, different factors are considered in one excavation site with the aim of testing the velocity equations based on actual field measurements, which finally results in different PPV values against the safe *MC* (23). To apply the controlled blasting techniques and to specify the relevant site-specific constants, many blasting data should be collected from the adjacent region (24, 25). In real conditions, the collected data are sometimes widely distributed and have a low correlation coefficient. In such cases, the equations obtained based on the assessment of these data typically demonstrate a low reliability level. Such unreliability is because of the variation in site-specific constants with direction (26, 27).

Recently, numerous soft computing (SC) methods have been introduced across the world. These tools help to find more accurate and authenticated solutions to complex problems that appear in engineering contexts. Such tools (28–34) have been developed and implemented by various scholars and practitioners working in different fields such as mining, civil engineering, geoengineering, and mechanics.

The prediction of blast-induced PPV has been done using several methods such as SC-based models. Ghasemi et al. (5) attempted to develop empirical models and a fuzzy model (FM) in order to predict the PPV value. To evaluate the model with the optimum performance, a number of performance indices, e.g., coefficient of determination (R^2), were proposed. According to their findings, an FM was capable of predicting PPV with a higher accuracy level in comparison with empirical equations. The FM recorded the R^2 value of 0.94, while for the empirical equations, this value was recorded as only 0.65. Furthermore, Radojica et al. (35) utilized empirical equations and an artificial neural network (ANN) to predict the PPV value. The final results showed a higher accuracy of the ANN, with $R^2 = 0.91$, compared to the empirical methods. To evaluate PPV, Hajihassani et al. (6) proposed a hybridization of an ANN with the imperialist competitive algorithm (ICA). Their results showed the R^2 values of 0.97, 0.91, and 0.87, obtained from the ICA-ANN, ANN, and MR models, respectively, which obviously indicates the higher effectiveness of the ICA-ANN compared to the other models. PPV in the study of Hasanipanah et al. (36) was estimated with the use of a genetic algorithm (GA). In separate studies, Hasanipanah et al. (37) and Jahed Armaghani et al. (7) made use of particle swarm optimization (PSO) and ICA, respectively, for the same objective, i.e., estimating the PPV value. Their findings showed the effectiveness of the GA, ICA, and PSO models in terms of developing non-linear equations applicable to the PPV prediction. The ANN performance was improved by Jahed Armaghani et al. (38, 39) and Hasanipanah et al. (40) by integrating it with optimization tools such as PSO. Taheri et al. (41) integrated an ANN with the artificial bee colony (ABC) algorithm as a way to estimate PPV. The comparative results showed the high capacity of an ABC in improving the performance quality of an ANN. Shahnazar et al. (42) predicted

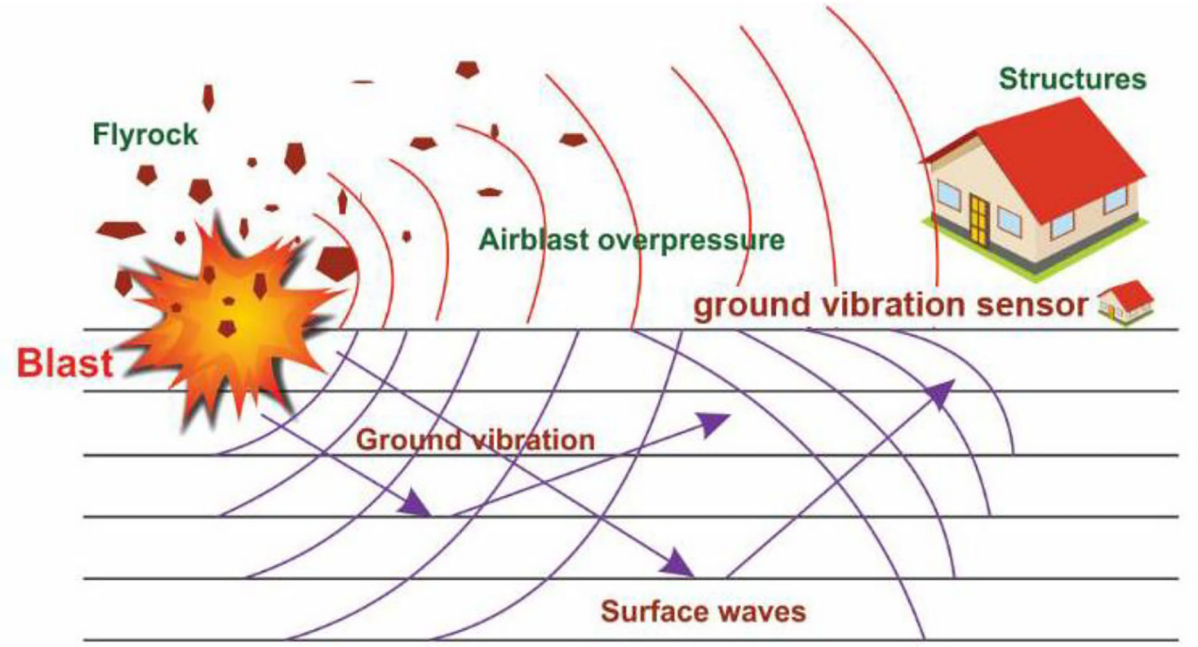

FIGURE 1
Phenomena induced by blasting (33).

PPV by integrating PSO with a neuro-fuzzy system. Their findings revealed the superiority of the hybrid model over the neuro-fuzzy system regarding PPV prediction. In Hasanipanah et al.'s (43) study, an ICA was combined with the fuzzy system (FS) and it was found successful in estimating the PPV value. In another research, Nguyen et al. (44) tested the random forest (RF) and extreme gradient boosting (XGBoost) models in terms of their effectiveness in estimating PPV. Findings confirmed that the XGBoost model was more successful than the rival regarding the defined task. In recent years, the Gaussian process regression (GPR) was investigated by Arthur et al. (8) regarding its accuracy in predicting ground vibration. According to their results, GPR had a higher capacity compared to empirical models in predicting PPV.

Recently, a novel SC approach was proposed by Zhang et al. (45) with the same objective. They utilized PSO in order to optimize the XGBoost. According to the results, if the PSO is effectively integrated with the XGBoost, the model's performance can be meaningfully improved. The boosted generalized additive models (BGAMs) were introduced by Nguyen et al. (10) with the aim of predicting PVV. They compared the results of their models with those of an ANN and a support vector machine (SVM). BGAMs were found practical and effective with results better than those of the ANN, SVM, and empirical models. Fang et al. (11), on the other hand, made use of an ICA for the purpose of optimizing the M5Rules model in estimating the PPV value. The findings confirmed that the ICA-M5Rules model was more successful than the conventional M5Rules, SVM, and RF models with regard to predicting PPV. Chandrahas et al. (46) used the K-Nearest Neighbor, XGBoost, and Random Forest models to predict PPV, and showed the effectiveness of XGBoost in this field compared to two other models. The gray wolf optimizer (GWO), as an optimization algorithm, was combined with an extreme learning machine (ELM) by Yan et al. (32) to predict PPV. They concluded the hybrid method was more effective and robust than the ELM and empirical models. The mentioned optimization algorithm was also combined with the relevance vector regression (RVR) with the same aim by Fattahi and Hasanipanah (33). For comparison purposes, a bat-inspired algorithm-RVR was used. The results confirmed that GWO-RVR performed better than the bat-inspired algorithm-RVR, which proved the effectiveness of GWO to improve the RVR model. In another hybrid model, a combination of an ANN and a Hunger Games Search (HGS) algorithm was tested by Nguyen and Bui (34) in terms of PPV prediction. In their study, three other optimization algorithms were also employed, and according to their results, the ANN-HGS model achieved more satisfactory predictive performance than the other models.

Zhang et al. (47) predicted PPV using chi-squared automatic interaction detection (CHAID), an RF, an ANN, an SVM, and classification and regression trees (CART). According to their results, the SVM yielded better performance for the prediction of PPV compared to others. Jahed Armaghani et al. (48)

10.3389/fpubh.2022.1094771

TABLE 1 Some studies in the field of PPV prediction.

References	SC technique	Input parameters
Khandelwal et al. (49)	SVM	Mc, Di
Dindarloo (50)	GEP	B, S, St, Mc, Di, radial distance, number, depth and diameter of holes
Saadat et al. (51)	ANN	Mc, Di, S, bench height
Taheri et al. (41)	ABC-ANN	Mc, Di
Mokfi et al. (52)	GMDH	B/S, hole depth, St, PF, Mc, Di
Azimi et al. (53)	GA-ANN	Mc, Di, radial distance, modified radial distance
Bui et al. (54)	PSO-KNN	Mc, Di
Chen et al. (55)	MFA-SVR	Mc, Di, B/S, St, E, Vp
Hasanipanah et al. (43)	FS-ICA	Mc, Di
Xue (56)	FCM-ANFIS	Mc, Di, scaled distance
Fang et al. (11)	ICA-M5Rules	Mc, Di, B, S
Hajihassani et al. (6)	ICA-ANN	B/S, St, Mc, Di, E
Amiri et al. (57)	ANN-KNN	Mc, Di
Sheykhi et al. (58)	FCM-SVR	B, S, St, number of holes per delay, Mc, Di
Yu et al. (59)	RVM	Mc, Di, B, vertical distance, Protodyakonovs impact strength coefficient, total explosive charged, delay time of detonator
Nguyen et al. (60)	GA-SVR-RBF	Mc, Di, B, S
Ding et al. (61)	ICA-XGBoost	Mc, Di, bench height, S, St, powder factor, B
Nguyen et al. (9)	HKM-CA	Mc, Di, bench height, powder factor, St, B, S
Zhou et al. (62)	FS-RF	S, B, Mc, Di, hole depth

B/S, burden to spacing ratio; St, Stemming; Vp, p-wave velocity; E, Young modulus; GEP, genetic expression programming; GMDH, group method of data handling; ANFIS, adaptive neuro-fuzzy inference system; KNN, k nearest neighbors; SVR, support vector regression; MFA, modified firefly algorithm; FCM, fuzzy Cmeans clustering; RBF, radial basis function; RVM, relevance vector machine; HKM-CA, hierarchical K-means clustering-cubist algorithm.

predicted PPV using a least square–SVM (LS–SVM), a GPR, a minimax probability machine regression (MPMR), and a PSO-extreme learning machine (PSO-ELM). The results indicated that the PSO-ELM was more computationally efficient with better predictive ability. Table 1 lists some studies in the field of PPV prediction.

In this study, the blast-induced PPV is predicted using a hybrid SC approach, called RSM-SVR, comprising two main regression techniques: the response surface model (RSM) and support vector regression (SVR). The proposed RSM-SVR model is structured using the RSM in the first calibrating process and SVR in the second calibrating process to improve the accuracy of the blast-induced PPV predictions. Then, the accuracy of the RSM-SVR model is compared with that of SVR, the RSM, and multivariate linear regression (MLR) based on several statistical factors. In addition, the PSO and GA, as two optimization algorithms, were employed and compared with the other models. The main contribution of this study to the body of knowledge is to propose a novel and efficient hybrid SC model, namely RSM-SVR, applicable in predicting blast-induced PPV.

The rest of this article includes the following. More details about the source of the datasets and also the hybrid SC model are explained in the second section. The results and discussions are provided in the third and fourth sections; then, the last section presents the conclusions of the study.

2. Materials and methods

2.1. Materials

The data used in this study were collected from the Harapan Ramai granite quarry located in the northern part of Johor, Malaysia. This quarry produces ~35,000–40,000 tons of granite aggregates per month. During each month, 8–10 blasting operations (depending on the weather condition) are performed. The main initiation and explosive materials are dynamite and ANFO, respectively. Fine gravel is used for the purpose of stemming the blast holes required.

For the purpose of this study, the parameters of *MC*, *B*, *S*, and *St* were measured before each blasting operation. Moreover, the block samples corresponding to each blast were transferred to the laboratory in order to measure the *Vp* and the unconfined compressive strength (*UCS*), according to ISRM (63). Based on the dataset collected, the burden-to-spacing ratio (*B/S*), *St*, *MC*, *E*, *Vp*, and *Di* were set as input variables.

In each blasting, PPV was recorded using the VibraZEB seismograph which possesses certain transducers for measuring PPV. In total, 90 blasts were monitored and the PPV in each event was calculated. The statistical characteristics of training and testing data sets for input variables are listed in Table 2. As indicated by the skewness results, the skewness does not follow the zero values for all data and almost all the variables tended to non-normal distributions. This means that the relations between PPV and almost all the input data can be described based on the non-linear form. As can be seen in Table 2, the skewness, STD, and mean of the database in the testing and training phases are assigned with different values for each variable of the input data set and PPV. The robustness and accuracy of predictions are more vital subjects for the validation of a model, which are learned using the data set in the training phase. The ability of a model to predict the non-linear relation is important

TABLE 2 Statistical characteristics of data sets.

Variables	Train phase						Test phase					
	X_{min}	X_{max}	Mean	STD	COV	Skewness	X_{min}	X_{max}	Mean	STD	COV	Skewness
Mc (kg)	133.59	534.37	345.970	131.387	0.380	−0.204	534.37	634.04	584.5004	28.776	0.049	−0.240
B/S	0.79	0.89	0.828	0.025	0.030	0.485	0.79	0.87	0.833	0.031	0.038	−0.026
St (m)	1.5	7	4.392	1.667	0.379	−0.244	7	8	7.32	0.379	0.052	0.688
E (GPa)	8.41	29.886	24.887	4.669	0.188	−1.877	19.606	29.748	24.965	3.220	0.129	−0.014
Vp (m/s)	2,805	4,506	3,769.446	525.157	0.139	−0.271	2,809	4,344	3,560.960	483.006	0.136	0.145
Di (m)	90	440	281.169	104.861	0.373	−0.560	195	430	334.040	62.618	0.187	−0.455
PPV(mm/s)	2.834	33.08	14.193	7.811	0.550	0.829	5.74	19.23	13.550	4.890	0.361	−0.400

in the current complex engineering problem. Thus, four non-linear models, i.e., MLR, RSM, SVR, and the proposed RSM-SVR are compared in terms of estimating PPV based on six input variables.

2.2. Methods

To achieve an accurate prediction of PPV, a novel SC method is herein proposed by integrating RSM with SVR models, i.e., RSM-SVR. The non-linear relation may be provided based on two regression processes of RSM and SVR between PPV and input factors. In this regard, RSM is combined with SVR based on two calibrating processes through which the input data of the proposed ML model is provided based on the RSM predictions. The structure of the hybrid RSM as input and SVR as an ML scheme (RSM-SVR) is plotted in Figure 2. As can be seen in this figure, the proposed RSM-SVR has three basic layers: (i) the input layer, (ii) the hidden layer [which is separated into two main layers, i.e., (1) predicted data set using RSM, and (2) the input data set using predicted data by RSM to provide the feature data in SVR], and (iii) the predicted layer using SVR. It is propsed that the input data set for SVR is provided based on the non-linear RSM relations that are predicted based on two individual input variables.

The input data sets, which are used to calibrate the response surface polynomial functions, should be selected with different input variables in the first calibrating process. Therefore, m–input data were prepared to calibrate the SVR provided based on the RSM by using n–input data. Thus, for the SVR model, n-dimension variables are transferred into m-dimension as follows:

$$m = \frac{n!}{2! \times (n-2)!} \tag{1}$$

where ! is the factorial operator. This model involves two main regression procedures: RSM and SVR. The former is used in the first stage, which can be extracted from the input data as presented in Figure 2. The m–input data provided in the hidden layer is computed using an RSM, which is a second-order polynomial function with cross-terms and two input variables (64, 65). Therefore, a simple non-linear relation is applied to estimate the m–hidden node using the RSM. The SVR prediction in the proposed method is dependent on the m–input data set. The input database-based estimated RSM is represented by a non-linear map ϕ_n with weights w_0-w_5 and two individual basic input data of x_i and x_j, as the following function:

$$\phi_n = w_0 + w_1 x_i + w_2 x_j + w_3 x_i^2 + w_4 x_j^2 + w_5 x_i x_j \tag{2}$$

The data set provided by non-linear map ϕ_n using the RSM provides the second-order non-linear relations with a linear correlation between input data as $x_i x_j$using Equation (2). ϕ_n $n = 1,2,\ldots, m$ has a similar dimension as well as PPV due to the use of RSM as the predictor of PPV. The last square estimator is applied to estimate the weights in Equation (2) as follows (66):

$$w = [P(X)^T P(X)]^{-1} [P(X)^T \begin{Bmatrix} x_i \\ x_j \end{Bmatrix}] \tag{3}$$

where,

$$P(X) = \begin{bmatrix} 1 & x_{i,1} & x_{j,1} & x_{i,1}^2 & x_{j,1}^2 & x_{i,1}x_{j,1} \\ 1 & x_{i,2} & x_{j,2} & x_{i,2}^2 & x_{j,2}^2 & x_{i,2}x_{j,2} \\ & \vdots & \vdots & \vdots & \vdots & \vdots \\ 1 & x_{i,N} & x_{j,N} & x_{i,N}^2 & x_{j,N}^2 & x_{i,N}x_{j,N} \end{bmatrix} \tag{4}$$

where i and j are the two input variables, and N represents the number of data points in the training phase. The data in the hidden nodes can be predicted using the weight. In the second process, using the m–input data provided by RSM, the SVR model is trained by the following relation (67):

$$y = b + \sum_{i=1}^{N} w_i K(\phi, \phi_i) \tag{5}$$

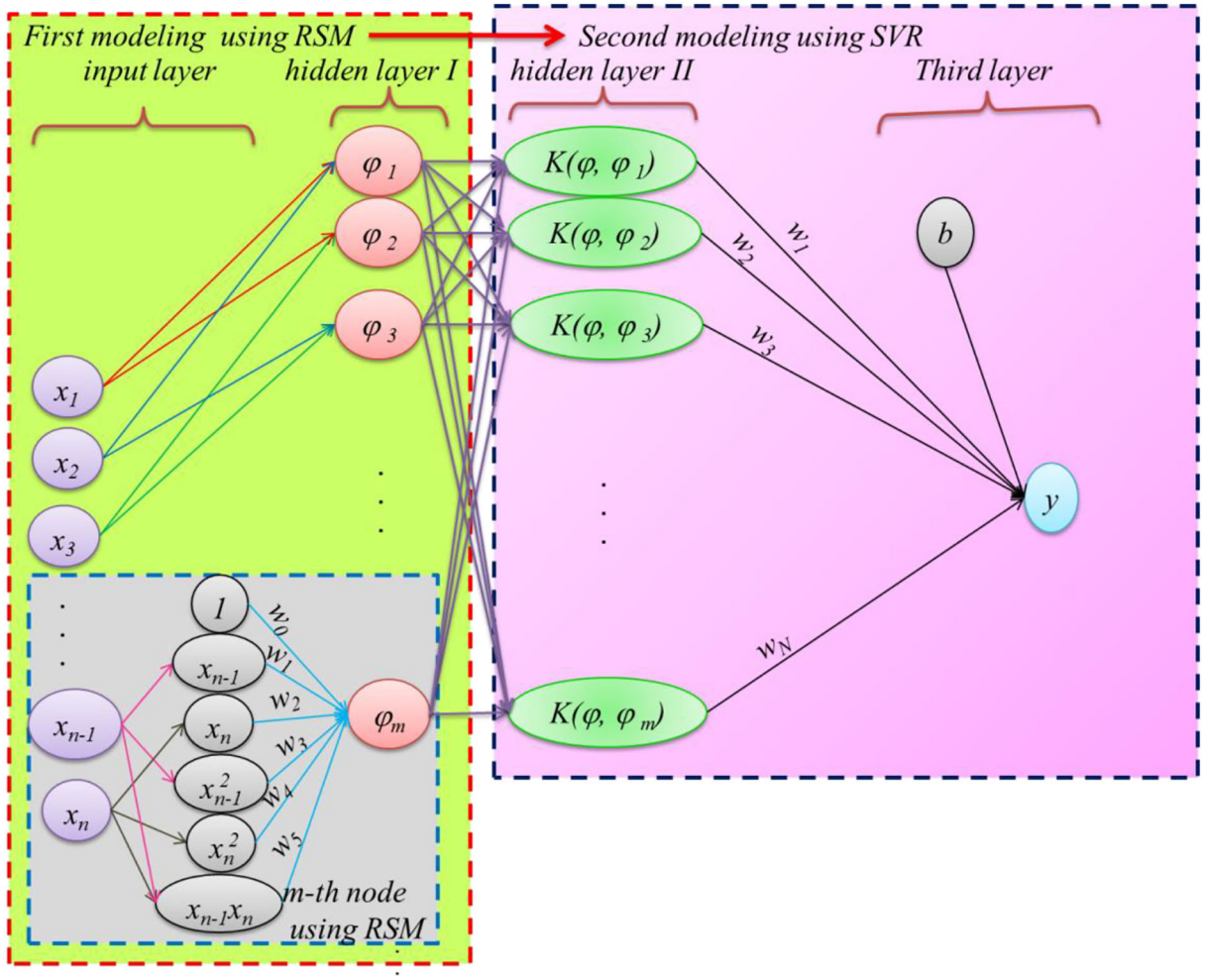

FIGURE 2
A view of RSM-SVR.

TABLE 3 Comparative error and agreement factors.

Methods	Train phase				Test phase				Time (s)
	MAE	RMSE	d	NSE	MAE	RMSE	d	NSE	
MLR	1.707	2.225	0.859	0.719	3.429	3.977	0.616	0.220	2.38
RSM	1.218	1.605	0.900	0.800	2.361	3.073	0.715	0.463	3.62
SVR	1.688	2.300	0.863	0.722	3.503	4.114	0.623	0.203	6.21
PSO-SVR	0.661	0.868	0.946	0.891	1.992	2.227	0.787	0.524	484.83
GA-SVR	1.397	1.780	0.886	0.770	2.152	2.837	0.741	0.480	543.41
RSM-SVR	0.061	0.296	0.995	0.990	1.379	1.619	0.832	0.686	8.94

where b is bias and $K(\phi, \phi_i)$ represents the Kernel function. The Gaussian kernel function is commonly implemented as follows (68–71):

$$K(\phi, \phi_i) = \exp(-0.5(\phi, \phi_i)^2/\sigma^2) \quad (6)$$

where σ denotes the parameter of kernel functions as $\sigma > 0$, which controls the smoothness of the kernel function. The weights of the N–feature data set in the SVR model are computed using the following model:

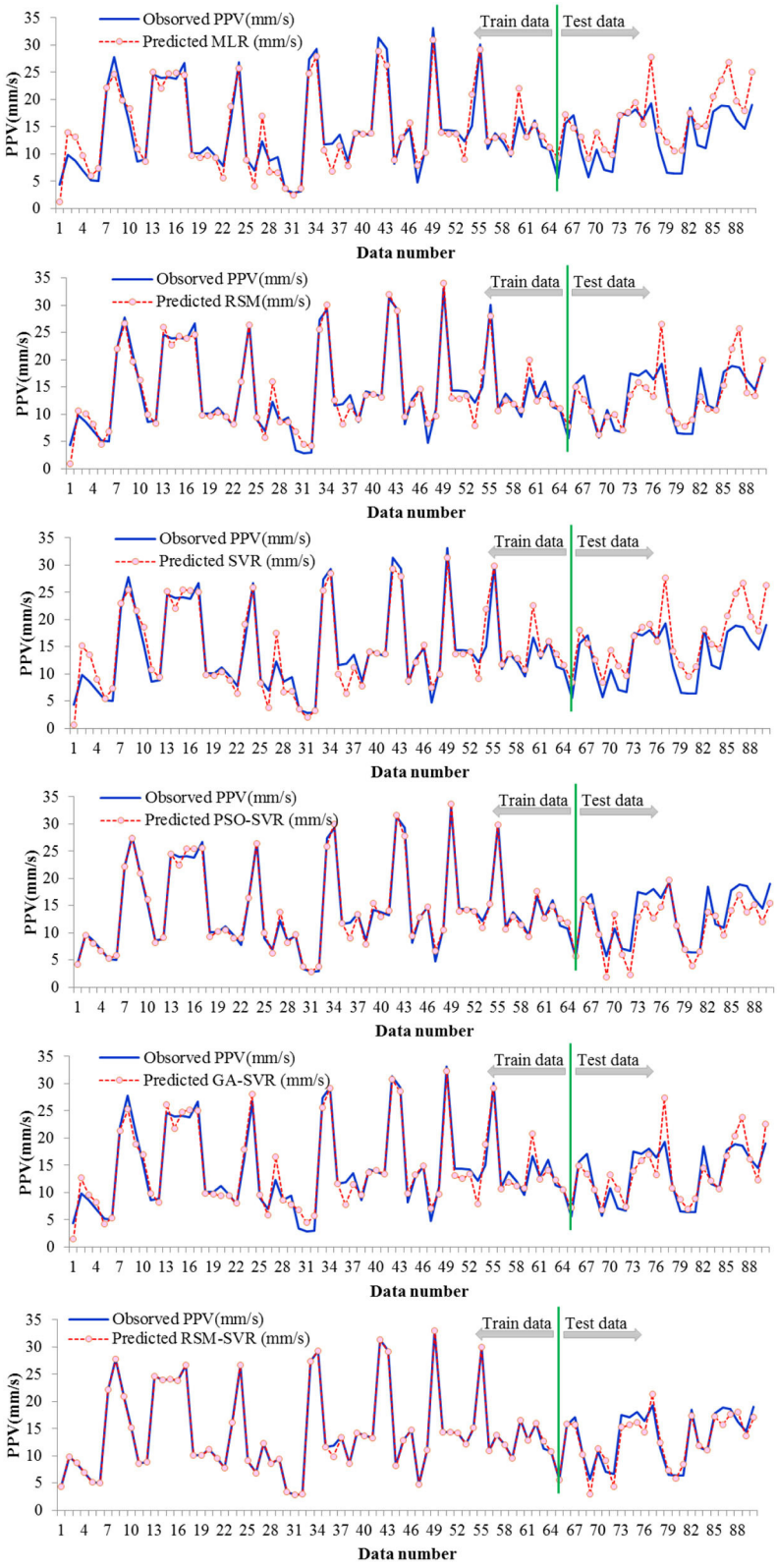

FIGURE 3
Comparison of predicted and observed data points of PPV for the developed models.

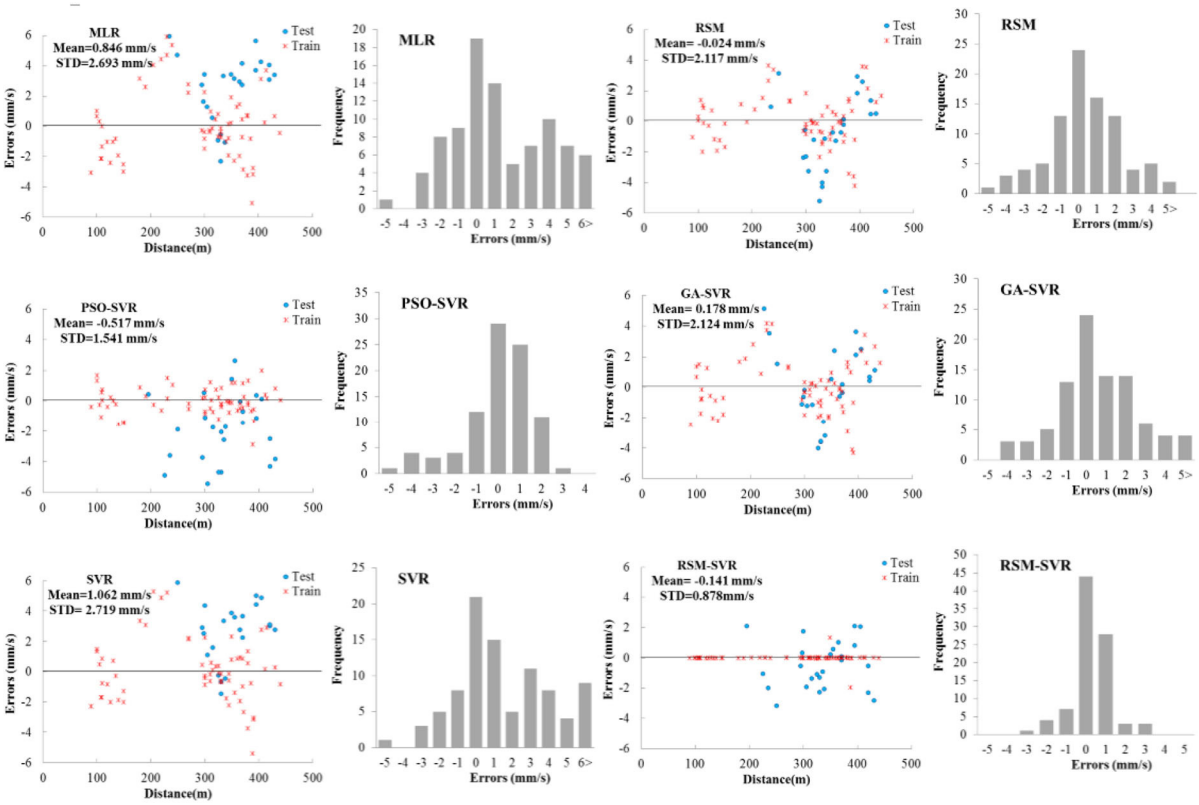

FIGURE 4
Errors (PPV_{exp}-PPV_{Pre}) of predictive models shown in bar diagrams, corresponding to distance.

$$Min \quad \frac{\|w\|^2}{2} + C\sum_{i=1}^{N}(\xi_i + \xi_i^*)$$
$$S.t. \quad \begin{cases} y_i - < w.K(x, x_i) > -b \le \varepsilon + \xi_i \\ < w.K(x, x_i) > +b - y_i \le \varepsilon + \xi_i^* \\ \xi_i, \xi_i^* \ge 0 \end{cases} \tag{7}$$

where ξ_i, ξ_i^* are the positive coefficients as errors, which are used to compute the errors of the predicted data using SVR ($w.K(x, x_i) + b$) and observed data (y_i);ε represents the ε-insensitive loss function to neglect the error less than ε. C is a positive factor. The SVR model is executed using parameters of ε, σ, and C which are given based on the trial-and-error method.

In addition, an RSM is a simple method to provide the non-linear polynomial relation (72). It is combined by SVR in the proposed learning approach. In an RSM, the data for input variables of SVR is predicted based on the least square method (73–75) in terms of the observed data, the two input data sets selected from *Mc, B/S, St, Di, E*, and *Vp*. The accuracy of predictions plays an essential role in designing and reliably evaluating the simulation of a complex engineering problem. The non-linear forms in the hidden nodes of the proposed method are considered by both Kernel relation and polynomial function. By applying two regression processes, the flexibility of the RSM is increased and then it can be applied to simulating and predicting non-linear problems such as the prediction of dissolved oxygen concentration (73), monthly pan evaporations (76), and the corroded burst pressure of pipelines (72). The *m*–data set provided by the RSM can be covered by the non-linear relations for complex problems, while the accuracy of prediction results using SVR in the next step is strongly improved by using the RSM to make non-linear input predictions. The proposed RSM-SVR machine learning model offers a high level of flexibility for predictions in non-linear problems. The regressed approach is presented by RSM-SVR based on the following steps:

1) Apply the RSM to the first calibrating stage as follows:

i) Give inputs ($x_1, x_2, \ldots, x_n$);
ii) Use two input variables from step (i) as input in the RSMs;
iii) Regress nodes of hidden layer 1 using the RSM by two input data sets provided by step (ii).

2) Apply the SVR to the second calibrating stage:

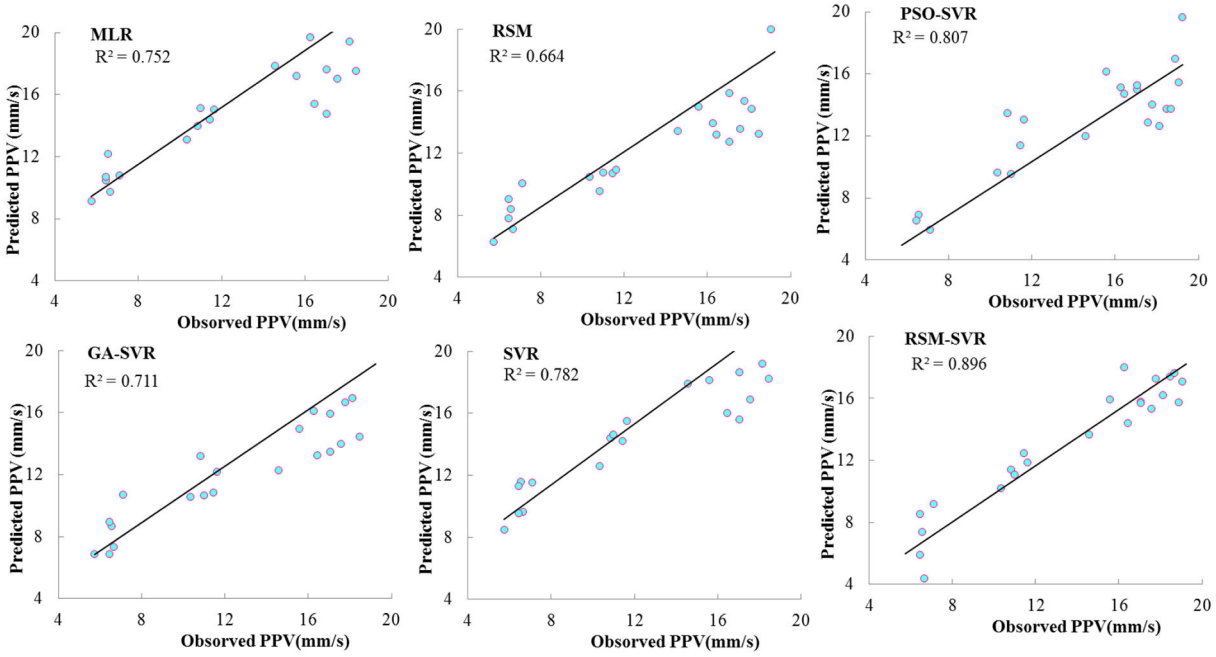

FIGURE 5
Scatterplot of predicted and observed PPV for test data set.

i) Give the input database to SVR from hidden layer 1;
ii) Select parameters for the SVR modeling procedure including ε, C, and σ;
iii) Train the SVR model using the input data set provided by RSM in the first calibrating stage.

3. Results

In this study, an MLR equation based on input parameters (*Mc*, *B/S*, *St*, *E*, *Vp*, and *Di*) and an output parameter (PPV) was constructed as follows:

$$PPV = 30.489 + 0.019Mc - \frac{3.585B}{S} + 0.0005St - 0.054E + 0.0004Vp - 0.074Di \quad (8)$$

Four statistical factors, i.e., mean absolute error (MAE), root mean square error (RMSE), Nash and Sutcliffe efficiency (*NSE*), and agreement index (d), are used to compare the performance of the MLR, RSM, SVR, and RSM-SVR models. The accuracy and agreement of the predictions for all the models are evaluated using the statistical factors presented in Equations (9)–(12) for both the testing and training data sets. By computing RMSE and MAE, the lower values represent the more accurate models, while higher NSE and d values indicate higher agreement predictions for a model. Therefore, the lowest values for error comparative factors, i.e., RMSE and MAE, and the highest agreement factor, i.e., d and NSE coefficients, can be used to select a model with superior prediction from among the other modeling approaches (77–87).

$$RMSE = \frac{1}{N}\sqrt{\sum_{i=1}^{N}[O_i - P_i]^2} \quad (9)$$

$$MAE = \frac{1}{N}\sum_{i=1}^{N}|O_i - P_i| \quad (10)$$

$$NSE = 1 - \frac{\sum_{i=1}^{N}|O_i - P_i|}{\sum_{i=1}^{N}|O_i - \overline{O}|}, \quad -\infty < NSE \leq 1 \quad (11)$$

$$d = 1 - \frac{\sum_{i=1}^{N}|O_i - P_i|}{\sum_{i=1}^{N}|O_i - \overline{O}| + |P_i - \overline{O}|}, \quad 0 < d \leq 1 \quad (12)$$

where N is the number of data in training (65 points) and testing (25 points) phases, O_i, P_i, and $\overline{O}$ are observed data, predicted i-th data, and mean of the observed data, respectively, which are computed as follows:

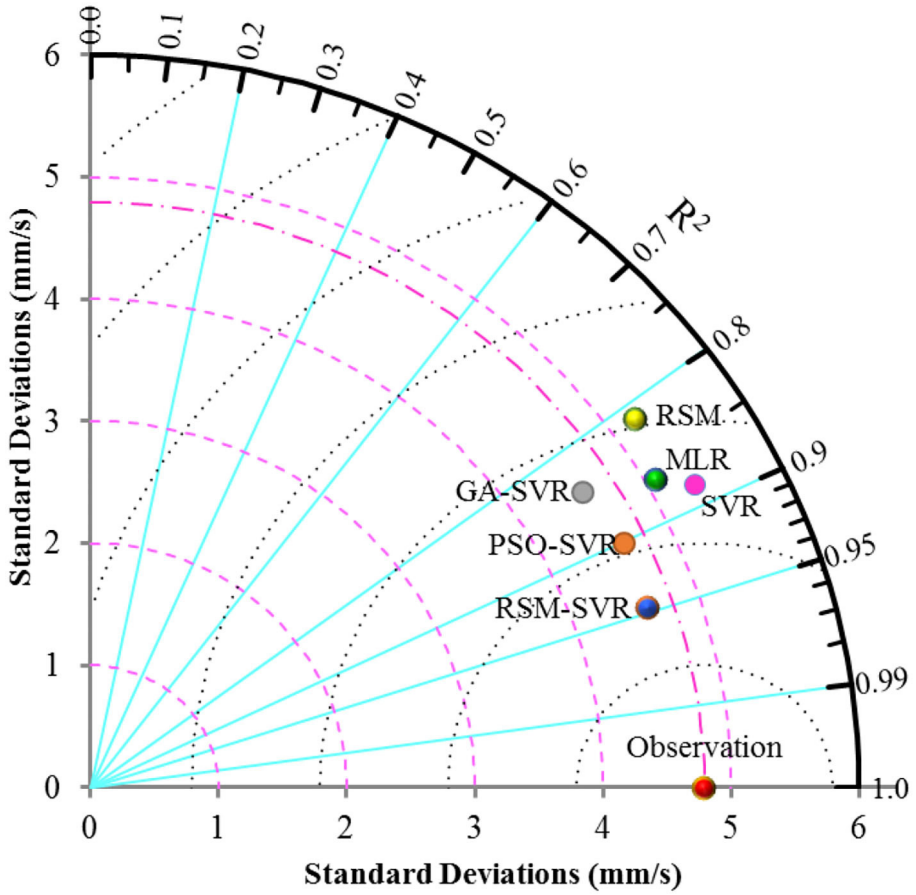

FIGURE 6
Taylor diagram for different models in the testing phase.

$$\overline{O} = \frac{\sum_{i=1}^{N} O_i}{N} \tag{13}$$

The experimental data sets used in this study are separated into two main categories: training and testing sets. The training points are used to build the relations using the MLR, RSM, and SVR models (with parameters as $\varepsilon = 0.05$, $\sigma = 1.25$, and $C = 1{,}000$), the RSM-SVR model (with SVR parameters: $\varepsilon = 0.02$, $\sigma = 1.15$, and $C = 1{,}500$), GA-SVR model (with GA parameters: number of generation = 500, number of population = 10, mutation = 0.025 and crossover percentage = 0.8) and PSO-SVR model (with PSO parameters: number of particles = 10, number of iterations = 500, inertia weight = 0.9, cognitive acceleration factor, i.e., $C_1 = 2$; social acceleration factor, i.e., $C_2 = 2$), while the testing points are used to validate the performance of the studied models in terms of accuracy. The errors of the predicted data points of $O_i - P_i$ (i.e., error = observed -predicted PPV) in the training and testing phases are compared to illustrate the robustness of the predictions of the studied models. Table 3 represents the comparative coefficients for both the training and testing data sets. Table 3 shows that the RSM-SVR model provided more accurate predictions than the other models for both the training and testing phases. In other words, this model obtained the lowest MAE and RMSE values and the highest d and NSE values. The proposed model was found to be as efficient as the SVR, and it strongly improved the computational B of the modeling process compared to the hybrid intelligent models of PSO-SVR and GA-SVR. The accuracy for decreasing the RMSE of the predicted PPV using the RSM-SVR model was enhanced by ~145%/650%, 90%/440%, 155%/670%, 74%/190%, and 75%/385% compared to the MLR, RSM, SVR, PSO-SVR, and GA-SVR models for training/testing, respectively. As can be seen, by applying a two-regression procedure provided by RSM in the first stage and SVR in the second one, the proposed method can significantly improve the accuracy of the perdition for the non-linear problem of predicting blast-induced ground vibrations. The hybrid optimization approaches

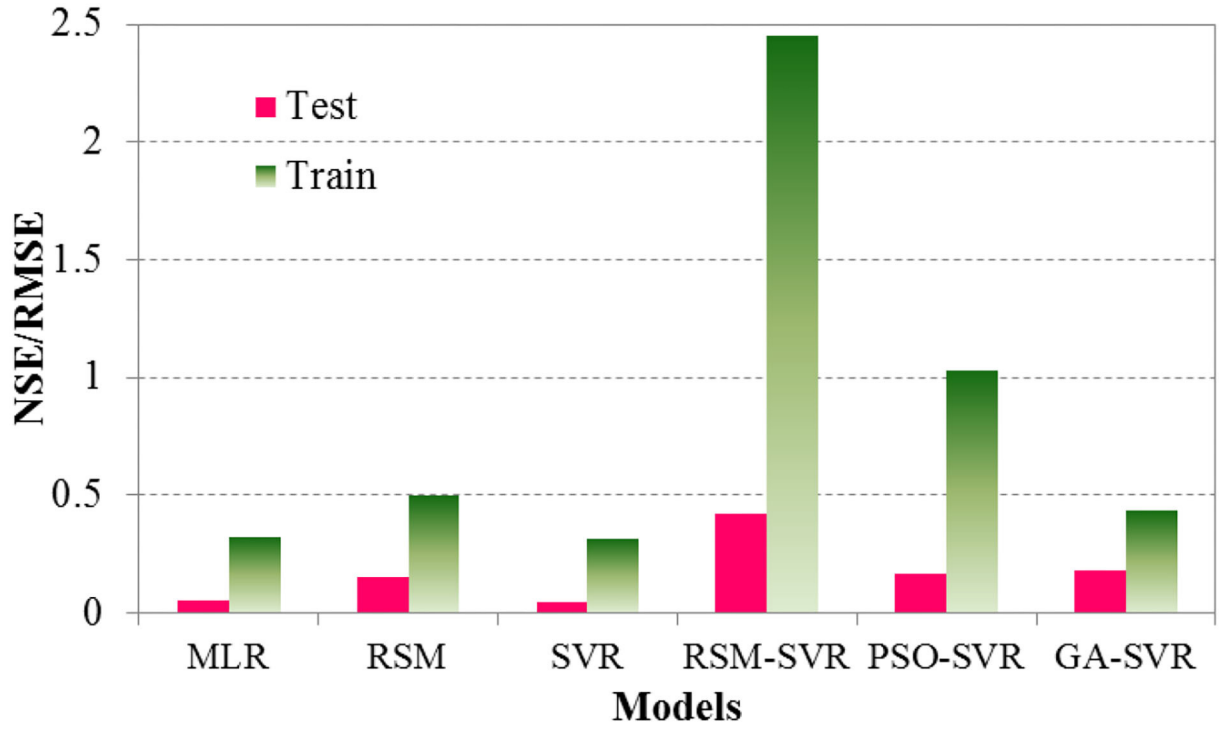

FIGURE 7
NSE/RMSE factors for different models in the training and testing phases.

integrating GA and PSO with SVR succeeded in further enhancing the capabilities of the predicted models compared to SVR and RSM.

The values of PPV for both predicted and observed PPV in the training and testing phases are plotted in Figure 3 for all studied models. This figure clearly reveals that the RSM-SVR model showed a superior predictive ability compared to the PSO-SVR, GA-SVR, SVR, RSM, and MLR models. This was because a good agreement between the predicted and experimental PPV values was obtained, shown by the highest d and NSE values presented in Table 3.

The errors observed-predicted data points of PPV, i.e., PPV_{exp}-PPV_{Pre}, were evaluated for developed models. The bar diagrams of errors and the scatter points for both the training and testing data sets with respect to the input variables of distance are presented in Figure 4. As this figure shows, the standard divisions (STD) for errors were obtained as 2.693, 2.217, 1.541, 2.124, 2.719, and 0.878 mm/s for the MLR, RSM, PSO-SVR, GA-SVR, SVR, and proposed RSM-SVR models, respectively. The MLR, RSM, and SVR models presented the predicted data with the same scatter. The distributed formats of the errors for these models are presented in error bars; the PSO-SVR model is offered among the models studied. The proposed model shows the perfect predictions for PVV in the training phase for almost all data points and its error bar shows narrower distributed bars compared to the PSO-SVR. This means that the proposed model has high flexibility to provide the non-linear relations for complex engineering problems, while the existing modeling approach based on MLR, GA-SVR, and SVR provides an error bar scattered similar to the regression approaches RSM. The hybridization approach to regression using the proposed RSM-SVR and PSO-SVR models enhances the predictions of complex engineering problems such as the PPV estimation.

Figure 5 shows the scatterplots for the predicted data points in the testing set corresponding to the observed PPV. According to this figure, the PSO-SVR, SVR, and RSM-SVR models provided relations of higher non-linearity compared to the MLR models with higher correlation coefficients: $R^2 = 0.896$ for RSM-SVR, $R^2 = 0.807$ for PSO-SVR, $R^2 = 0.782$ for SVR, the MLR with $R^2 = 0.752$, and GA-SVR with $R^2 = 0.711$. Consequently, it can be concluded that the flexible non-linear relations are provided based on two regression phases in the proposed models, while other comparative models are established based on one regression phase. The non-linear map using the RSM as input variables provides an acceptable input variable for the prediction of SVR in the proposed hybrid model for accurate predictions of PPV. The RSM shows the prediction results with the lowest accuracy, $R^2 = 0.664$, while the non-linearity degree of the RSM is more than MLR but still does not show the acceptable flexibility for modeling this problem with

less error than MLR. Due to the high flexibility in providing the non-linear relation, the accuracy of the proposed RSM-SVR model is strongly improved compared to the SVR, GA-SVR, and RSM models. The proposed model strongly improved the prediction performance of the RSM for this complex problem.

4. Discussion

To have a better discussion about the accuracy and agreement of the models, the Taylor diagram was used and the NSE/RMSE of the developed models were taken into consideration. The Taylor diagram is used by standard deviations and R^2 of predicted results for different models can show the models performance. The NSE/RMSE is computed based on the comparative statistics, which can be used for measuring accuracy (i.e., RMSE) and agreement (i.e., NSE). The larger the NSE/RMSE value, the superior the performance of the model. The Taylor diagrams for the RSM, MLR, SVR, PSO-SVR, GA-SVR, and RSM-SVR models with observed data (represented by the red point on the horizontal line as observation) are presented in Figure 6, for the testing database. The NSE/RMSE results for different models in the testing and training data sets are shown in Figure 7.

Figure 6 and the NSE/RMSE ratios presented in Figure 7 indicate that the models have performed differently in accuracy and agreement. SVR offered higher agreement than MLR and the RSM, while it showed less agreement than the PSO-SVR, GA-SVR, and RSM-SVR models. MLR and the RSM-SVR showed close standard deviations compared to the others. The RSM-SVR offered more accurate predictions than the other models and it showed a higher agreement compared to the SVR, GA-SVR, RSM, and MLR models for the complex problem at hand. The optimization method for tuning the parameters of the hybrid SVR models (i.e., ε, C, and σ) of PSO-SVR can improve the capabilities of SVR models for this problem. By comparing the results represented by the Taylor diagram, the models were ranked from best to worst as follows: (1) RSM-SVR, (2) PSO-SVR, (3) GA-SVR, (4) SVR, (5) MLR, and (6) RSM.

The capabilities of the proposed hybrid SVR method in terms of both agreement and accuracy were enhanced using two regression procedures. The data handling set as input (which was provided by the RSM) was used for the training process of the SVR model, while the main objective for hybridizing the SVR with the optimization methods of PSO (PSO-SVR) and GA (GA-SVR) was to find the best parameters of the SVR model. The use of optimization algorithms in the PSO-SVR and GA-SVR models causes them to consume more computation time than the RSM-SVR model. By comparing the RSM-SVR model with hybrid intelligent models of PSO-SVR and GA-SVR, the main advantages of the RSM-SVR model is the use of only one process for the SVR model regression and also the use of the handling input data computed by RSM. In future research, the proposed model and the models hybridizing SVR with optimization methods can enhance the quality of prediction in complex engineering problems.

It is worth mentioning that the performance of a predictor is significantly related to the database used as well as the type of rock. The field investigated in this study is a granite quarry located in Malaysia. By reviewing the previous studies, it was found that Zhang et al. (47), Jahed Armaghani et al. (48), and Zhou et al. (88) have previously conducted studies on the prediction of PPV in granite quarries located in this country. Therefore, the performance of the proposed RSM-SVR presented in this study can be compared with that of the models developed in the aforementioned studies. According to Zhang et al. (47), the PPV was predicted by CHAID, RF, ANN, SVM, and CART models. Based on their results, the values of R^2 obtained from CHAID, RF, ANN, SVM, and CART models were equal to 0.68, 0.83, 0.84, 0.85, and 0.56, respectively. In the study conducted by Jahed Armaghani et al. (48), the LS–SVM, GPR, MPMR, and PSO- PSO-ELM models were employed. They developed three autonomous groups of PSO (AGPSO) models in combination with ELM. They showed the values of R^2 in the range of 0.8–0.89 for the MPMR, LS–SVM, GPR, PSO-ELM, AGPSO1–ELM, AGPSO2–ELM, and AGPSO3–ELM models, respectively. Furthermore, Zhou et al. (88) predicted PPV using five different gene expression programming (GEP) models, and in the best model, the value of R^2 was equal to 0.88. The RSM-SVR model proposed in this study predicted PPV with an R^2 of 0.896 ($\sim$ 0.9). A comparison with the results of the above-mentioned models indicates the effectiveness of the RSM-SVR model in predicting PPV.

In this study, a sensitivity analysis was also performed to check the level of input parameters' intensity on the output parameter (PPV) through the following equation from Yang and Zhang (89):

$$r_{ij} = \frac{\sum_{k=1}^{n} (y_{ik} \times y_{ok})}{\sqrt{\sum_{k=1}^{n} y_{ik}{}^2 \sum_{k=1}^{n} y_{ok}{}^2}} \quad (14)$$

where y_i and y_o are the input and output parameters, respectively. The parameter with the highest r_{ij} has the highest effect on output. According to the results, the r_{ij} values for the *Di, Vp, E, St, B/S*, and *Mc* were 0.729, 0.891, 0.877, 0.838, 0.892, and 0.839, respectively. Therefore, the *Vp* and *B/S* were identified as the most effective parameters on PPV.

5. Conclusions

The accurate prediction of PPV is of high importance to safety issues in surface mines. This study aimed to propose a novel hybrid SC model, namely the RSM-SVR model. This model is structured using an RSM in the first calibrating process

and an SVR in the second calibrating process to improve the accuracy of the PPV predictions. In addition, SVR, SVR-PSO, SVR-GA, RSM, and MLR models were also used in this study for comparison purposes. The above-mentioned models were developed to predict PPV in a granite quarry located in Johor, Malaysia. To this end, 90 blasting events were monitored and the values of *B, S, St, Mc, Di, E*, and *Vp* were precisely measured. In addition, the obtained PPV values for each blasting event were recorded. After constructing the models, four statistical factors, namely MAE, RMSE, NSE, and d were implemented to check the performance of the models. Finally, the following conclusions were drawn from this study:

- Experimental results demonstrated that the RSM-SVR model achieved the greatest evaluation criteria for R^2 (0.896), MAE (1.379 mm/s), RMSE (1.619 mm/s), d (0.832), and NSE (0.686).
- Comparing the results, it was found that the RSM-SVR model provided a prediction of relatively higher accuracy than that of the PSO-SVR, GA-SVR, MLR, SVR, and RSM models.
- Hybridizing the SVR and an RSM is a powerful approach to solving prediction-based problems and has the capacity to be generalized to other fields.
- According to the sensitivity analysis, the *Vp* and *B/S*, were the most effective parameters on the PPV.

To end with, future research directions include, but are not limited to, the following: (1) applying the RSM-SVR model to other prediction problems in the fields of mining and geotechnical engineering; and (2) using other optimization algorithms such as the variable depth search algorithm, cultural algorithm, water flow-like algorithm, cyber swarm algorithm, water wave optimization, and jaguar algorithm to improve the SVR performance.

Data availability statement

The original contributions presented in the study are included in the article/supplementary material, further inquiries can be directed to the corresponding author.

Author contributions

Conceptualization and data curation: MH. Methodology and validation: BK and JP. Investigation: JP and BN. Writing—original draft preparation and writing—review and editing: BK, JP, RA, MH, MM, and BN. Supervision: MH and RA. Funding acquisition: MM. All authors have read and agreed to the published version of the manuscript.

Funding

This research was partially funded by the Ministry of Science and Higher Education of the Russian Federation, under the strategic academic leadership program Priority 2030 (Agreement 075-15-2021-1333, dated September 30, 2021).

Acknowledgments

The authors would like to thank Dr. Jahed Armaghani for providing the information and facilities required for conducting this research.

Conflict of interest

The authors declare that the research was conducted in the absence of any commercial or financial relationships that could be construed as a potential conflict of interest.

Publisher's note

References

1. Singh TN, Dontha LK, Bhardwaj V. Study into blast vibration and frequency using ANFIS and MVRA. *Mining Technol.* (2008) 117:116–21. doi: 10.1179/037178409X405741

2. Khandelwal M, Singh TN. Prediction of blast induced air overpressure in opencast mine. *Noise Vib Control Worldw.* (2005) 36:7–16. doi: 10.1260/0957456053499095

3. Khandelwal M, Singh TN. Prediction of blast-induced ground vibration using artificial neural network. *Int J Rock Mech Mining Sci.* (2009) 46:1214–22. doi: 10.1016/j.ijrmms.2009.03.004

4. Monjezi M, Hasanipanah M, Khandelwal M. Evaluation and prediction of blast-induced ground vibration at Shur River Dam, Iran, by artificial neural network. *Neural Comput Appl.* (2013) 22:1637–43. doi: 10.1007/s00521-012-0856-y

5. Ghasemi E, Ataei M, Hashemolhosseini H. Development of a fuzzy model for predicting ground vibration caused by rock blasting in surface mining. *J Vib Control.* (2013) 19:755–70. doi: 10.1177/1077546312437002

6. Hajihassani M, Jahed Armaghani D, Marto A, Mohamad ET. Ground vibration prediction in quarry blasting through an artificial neural network optimized

by imperialist competitive algorithm. *Bull Eng Geol Environ.* (2015) 74:873–86. doi: 10.1007/s10064-014-0657-x

7. Jahed Armaghani D, Hasanipanah M, Amnieh HB, Mohamad ET. Feasibility of ICA in approximating ground vibration resulting from mine blasting. *Neural Comput Appl.* (2018) 29:457–65. doi: 10.1007/s00521-016-2577-0

8. Arthur CK, Temeng VA, Ziggah YY. Novel approach to predicting blast-induced ground vibration using Gaussian process regression. *Eng Comput.* (2019) 36:29–42. doi: 10.1007/s00366-018-0686-3

9. Nguyen H, Bui XN, Tran QH, Mai NL. A new soft computing model for estimating and controlling blast-produced ground vibration based on hierarchical K-means clustering and Cubist algorithms. *Appl Soft Comput.* (2019) 77:376–86. doi: 10.1016/j.asoc.2019.01.042

10. Nguyen H, Bui XN, Tran QH, Moayedi H. Predicting blast-induced peak particle velocity using BGAMs, ANN and SVM: a case study at the Nui Beo open-pit coal mine in Vietnam. *Environ Earth Sci.* (2019) 78:479. doi: 10.1007/s12665-019-8491-x

11. Fang Q, Nguyen H, Bui XN, Nguyen-Thoi T. Prediction of blast-induced ground vibration in open-pit mines using a new technique based on imperialist competitive algorithm and M5Rules. *Nat Resour Res.* (2019) 29:791–806. doi: 10.1007/s11053-019-09577-3

12. Nguyen H, Drebenstedt C, Bui XN, Bui DT. Prediction of blast-induced ground vibration in an open-pit mine by a novel hybrid model based on clustering and artificial neural network. *Nat Resour Res.* (2019) 29:691–709. doi: 10.1007/s11053-019-09470-z

13. Yang H, Hasanipanah M, Tahir MM, Bui DT. Intelligent prediction of blasting-induced ground vibration using ANFIS optimized by GA and PSO. *Nat Resour Res.* (2019) 29:739–50. doi: 10.1007/s11053-019-09515-3

14. Zhu W, Nikafshan Rad H, Hasanipanah M. A chaos recurrent ANFIS optimized by PSO to predict ground vibration generated in rock blasting. *Appl Soft Comput.* (2021) 108:107434. doi: 10.1016/j.asoc.2021.107434

15. Ozer U. Environmental impacts of ground vibration induced by blasting at different rock units on the Kadikoy–Kartal metro tunnel. *Eng Geol.* (2008) 100:82–90. doi: 10.1016/j.enggeo.2008.03.006

16. Nateghi R. Evaluation of blast induced ground vibration for minimizing negative effects on surrounding structures. *Soil Dyn Earthquake Eng.* (2012) 43:133–8. doi: 10.1016/j.soildyn.2012.07.009

17. Nateghi R, Kiany M, Gholipouri M. Control negative effects of blasting waves on concrete of the structures by analyzing of parameters of ground vibration. *Tunneling Underground Space Technol.* (2009) 24:608–16. doi: 10.1016/j.tust.2009.04.004

18. Sivarajan V, Kumara K, Hearath H. Ground vibration and air blast over-pressure assessment using scaled distance. In: *Proceedings of Environmental Research Event. Auckland, New Zealand.* (2007). p. 6–33.

19. Ghosh A, Daemen JK. A simple new blast vibration predictor. In: *Proceedings of the 24th US Symp on Rock Mechanics. College Station, TX, USA.* (1983). p. 151–61.

20. Gupta RN, Roy PP, Bagachi A, Singh B. Dynamic effects in various rock mass and their predictions. *J Mines Met Fuels.* (1987) 35:455–62.

21. Gupta RN, Roy PP, Singh B. On a blast induced blast vibration predictor for efficient blasting. In: *Proc 22nd Int Conf of Safety in Mines, Beijing, China, 2–6 Nov 1987.* (1988). p. 1015–21.

22. Roy PP. Vibration control in an opencast mine based on improved blast vibration predictors. *Min Sci Tech.* (1991) 12:157–65. doi: 10.1016/0167-9031(91)91642-U

23. Arpaz E, Uysal O, Tola Y, Gorgulu K, C, avus, M. Comparison of blast-induced ground vibration predictors in Seyitomer coal mine. In: *12th Rock Mechanics Symp, Beijing, China, 18-21 October 2011.* (2012). p. 1161–3.

24. ISRM. Suggested method for blast vibration monitoring. *Int J Rock Mech Mining Sci Geo Abs.* (1992) 29:143–56. doi: 10.1016/0148-9062(92)92124-U

25. Arpaz E. Monitoring and evaluation of blast induced vibrations in some open-pit mines in Turkey (Dissertation) Cumhuriyet University, Sivas (in Turkish) (2000).

26. Jimeno CL, Jimeno EL, Carcedo FJA. *Drilling and Blasting of Rocks*. Rotterdam A.A. Balkema (1995). p. 390.

27. Aldas GGU. Effect of some rock mass properties on blasting induced ground vibration wave characteristics at Orhaneli surface coal mine. (Dissertation) Middle East Technical University, Ankara, Turkey (2002).

28. Nguyen H, Bui XN. Optimized adaptive neuro-fuzzy inference system for predicting blast-induced ground vibration in quarries based on hunger games search optimization. *Int J Min Reclam Environ.* (2022) 36:724–48. doi: 10.1080/17480930.2022.2131137

29. Temeng VA, Arthur CK, Ziggah YY. Suitability assessment of different vector machine regression techniques for blast-induced ground vibration prediction in Ghana. *Model Earth Syst Environ.* (2022) 8:897–909. doi: 10.1007/s40808-021-01129-0

30. Hasanipanah M, Jamei M, Mohammed AS, Nait Amar M, Hocine O, Khedher KM. Intelligent prediction of rock mass deformation modulus through three optimized cascaded forward neural network models. *Earth Sci Inform.* (2022) 15:1659–69. doi: 10.1007/s12145-022-00823-6

31. Asteris PG, Mamou A, Hajihassani M, Hasanipanah M, Koopialipoor M, Le TT, et al. Soft computing based closed form equations correlating L and N-type Schmidt hammer rebound numbers of rocks. *Transp Geotech.* (2021) 29:100588. doi: 10.1016/j.trgeo.2021.100588

32. Yan Y, Hou X, Cao S, Li R, Zhou W. Forecasting the collapse-induced ground vibration using a GWO-ELM model. *Buildings.* (2022) 12:121. doi: 10.3390/buildings12020121

33. Fattahi H, Hasanipanah M. Prediction of blast-induced ground vibration in a mine using relevance vector regression optimized by metaheuristic algorithms. *Nat Resour Res.* (2021) 30:1849–63. doi: 10.1007/s11053-020-09764-7

34. Nguyen H, Bui XN. A novel hunger games search optimization-based artificial neural network for predicting ground vibration intensity induced by mine blasting. *Nat Resour Res.* (2021) 30:3865–80. doi: 10.1007/s11053-021-09903-8

35. Radojica L, Kostic' S, Pantovic' R, Vasovic' N. Prediction of blast-produced ground motion in a copper mine. *Int J Rock Mech Min Sci.* (2014) 69:19–25. doi: 10.1016/j.ijrmms.2014.03.002

36. Hasanipanah M, Golzar SB, Larki IA, Maryaki MY, Ghahremanians T. Estimation of blast-induced ground vibration through a soft computing framework. *Eng Comput.* (2017) 33:951–9. doi: 10.1007/s00366-017-0508-z

37. Hasanipanah M, Naderi R, Kashir J, Noorani SA, Aaq Qaleh AZ. Prediction of blast produced ground vibration using particle swarm optimization. *Eng Comput.* (2017) 33:173–9. doi: 10.1007/s00366-016-0462-1

38. Jahed Armaghani D, Hajihassani M, Mohamad ET, Marto A, Noorani SA. Blasting-induced flyrock and ground vibration prediction through an expert artificial neural network based on particle swarm optimization. *Arab J Geosci.* (2014) 7:5383–96. doi: 10.1007/s12517-013-1174-0

39. Jahed Armaghani D, Raja SNSB, Faizi K, Rashid ASA. Developing a hybrid PSO–ANN model for estimating the ultimate bearing capacity of rock-socketed piles. *Neural Comput Appl.* (2015) 28:391–405. doi: 10.1007/s00521-015-2072-z

40. Hasanipanah M, Noorian-Bidgoli M, Armaghani DJ, Khamesi H. Feasibility of PSO-ANN model for predicting surface settlement caused by tunneling. *Eng Comput.* (2016) 32:705–15. doi: 10.1007/s00366-016-0447-0

41. Taheri K, Hasanipanah M, Bagheri Golzar S, Majid MZA. A hybrid artificial bee colony algorithm-artificial neural network for forecasting the blast-produced ground vibration. *Eng Comput.* (2016) 33:689–700. doi: 10.1007/s00366-016-0497-3

42. Shahnazar A, Rad HN, Hasanipanah M, Tahir MM, Armaghani DJ, Ghoroqi M. A new developed approach for the prediction of ground vibration using a hybrid PSO-optimized ANFIS-based model. *Environ Earth Sci.* (2017) 76:527. doi: 10.1007/s12665-017-6864-6

43. Hasanipanah M, Bakhshandeh Amnieh H, Khamesi H, Jahed Armaghani D, Bagheri Golzar S, Shahnazar A. Prediction of an environmental issue of mine blasting: an imperialistic competitive algorithm-based fuzzy system. *Int J Environ Sci Technol.* (2018) 15:551–60. doi: 10.1007/s13762-017-1395-y

44. Nguyen H, Bui XN, Bui HB, Cuong DT. Developing an XGBoost model to predict blast-induced peak particle velocity in an open-pit mine: a case study. *Acta Geophysica.* (2019) 67:477–90. doi: 10.1007/s11600-019-00268-4

45. Zhang X, Nguyen H, Bui XN, Tran QH, Nguyen DA, Tien Bui D, et al. Novel soft computing model for predicting blast-induced ground vibration in open-pit mines based on particle swarm optimization and XGBoost. *Natural Resources Res.* (2019) 29:711–21. doi: 10.1007/s11053-019-09492-7

46. Chandrahas NS, Choudhary BS, Teja MV, Venkataramayya MS, Prasad NSRK. XG boost algorithm to simultaneous prediction of rock fragmentation and induced ground vibration using unique blast data. *Appl Sci.* (2022) 12:5269. doi: 10.3390/app12105269

47. Zhang H, Zhou J, Jahed Armaghani D, Tahir MM, Pham BT, Huynh VV. A combination of feature selection and random forest techniques to solve a problem related to blast-induced ground vibration. *Appl Sci.* (2020) 10:869. doi: 10.3390/app10030869

48. Jahed Armaghani D, Kumar D, Samui P, Hasanipanah M, Roy B. A novel approach for forecasting of ground vibrations resulting from blasting: modified particle swarm optimization coupled extreme learning machine. *Eng Comput.* (2020) 37:3221–35. doi: 10.1007/s00366-020-00997-x

49. Khandelwal M, Kankar P, Harsha S. Evaluation and prediction of blast induced ground vibration using support vector machine. *Min Sci Technol.* (2010) 20:64–70. doi: 10.1016/S1674-5264(09)60162-9

50. Dindarloo SR. Prediction of blast-induced ground vibrations via genetic programming. *Int J Min Sci Technol.* (2015) 25:1011–15. doi: 10.1016/j.ijmst.2015.09.020

51. Saadat M, Khandelwal M, Monjezi M. An ANN based approach to predict blast-induced ground vibration of Gol-E-Gohar iron ore mine, Iran. *J Rock Mech Geotech Eng.* (2014) 6:67–76. doi: 10.1016/j.jrmge.2013.11.001

52. Mokfi T, Shahnazar A, Bakhshayeshi I, Derakhsh AM, Tabrizi O. Proposing of a new soft computing-based model to predict peak particle velocity induced by blasting. *Eng Comput.* (2018) 34:881–8. doi: 10.1007/s00366-018-0578-6

53. Azimi Y, Khoshrou SH, Osanloo M. Prediction of blast induced ground vibration (BIGV) of quarry mining using hybrid genetic algorithm optimised artificial neural network. *Measurement.* (2019) 147:106874. doi: 10.1016/j.measurement.2019.106874

54. Bui XN, Jaroonpattanapong P, Nguyen H, Tran QH, Long NQ. A novel hybrid model for predicting blast-induced ground vibration based on k-nearest neighbors and particle Swarm optimisation. *Sci Rep.* (2019) 9:1–14. doi: 10.1038/s41598-019-50262-5

55. Chen W, Hasanipanah M, Rad HN, Armaghani DJ, Tahir M. A new design of evolutionary hybrid optimization of SVR model in predicting the blast-induced ground vibration. *Eng Comput.* (2019) 37:1455–71. doi: 10.1007/s00366-019-00895-x

56. Xue X. Neuro-fuzzy based approach for prediction of blast-induced ground vibration. *Appl Acoust.* (2019) 152:73–8. doi: 10.1016/j.apacoust.2019.03.023

57. Amiri M, Amnieh HB, Hasanipanah M, Khanli LM. A new combination of artificial neural network and K-nearest neighbors models to predict blast-induced ground vibration and air-overpressure. *Eng Comput.* (2016) 32:631–44. doi: 10.1007/s00366-016-0442-5

58. Sheykhi H, Bagherpour R, Ghasemi E, Kalhori H. Forecasting ground vibration due to rock blasting: a hybrid intelligent approach using support vector regression and fuzzy C-means clustering. *Eng Comput.* (2018) 34:357–65. doi: 10.1007/s00366-017-0546-6

59. Yu Z, Shi X, Zhou J, Gou Y, Huo X, Zhang J et al. A new multikernel relevance vector machine based on the HPSOGWO algorithm for predicting and controlling blast-induced ground vibration. *Eng Comput.* (2020) 38:1905–20. doi: 10.1007/s00366-020-01136-2

60. Nguyen H, Choi Y, Bui XN, Nguyen Thoi T. Predicting blast-induced ground vibration in open-pit mines using vibration sensors and support vector regression-based optimisation algorithms. *Sensors.* (2019) 20:132. doi: 10.3390/s20010132

61. Ding Z, Nguyen H, Bui XN, Zhou J, Moayedi H. Computational intelligence model for estimating intensity of blast-induced ground vibration in a mine based on imperialist competitive and extreme gradient boosting algorithms. *Natural Resources Res.* (2019) 29:751–69. doi: 10.1007/s11053-019-09548-8

62. Zhou J, Asteris PG, Armaghani DJ, Pham BT. Prediction of ground vibration induced by blasting operations through the use of the Bayesian Network and random forest models. *Soil Dyn Earthquake Eng.* (2020) 139:106390. doi: 10.1016/j.soildyn.2020.106390

63. ISRM. The complete ISRM suggested methods for rock characterization, testing and monitoring 2007: 1974–2006. In: Ulusay R, Hudson JA, editors. *Suggested Methods Prepared by the Commission on Testing Methods*. International Society for Rock Mechanics. ISRM Turkish National Group, Ankara, Turkey.

64. Fei CW, Li H, Liu HT, Lu C, Keshtegar B. Multilevel nested reliability-based design optimization with hybrid intelligent regression for operating assembly relationship. *Aerospace Sci Technol.* (2020) 103:105906. doi: 10.1016/j.ast.2020.105906

65. Xiao M, Zhang J, Gao L. A system active learning Kriging method for system reliability-based design optimization with a multiple response model. *Reliability Eng Syst Saf.* (2020) 199:106935. doi: 10.1016/j.ress.2020.106935

66. Fei CW, Lu C, Liem RP. Decomposed-coordinated surrogate modeling strategy for compound function approximation in a turbine-blisk reliability evaluation. *Aerospace Sci Technol.* (2019) 95:105466. doi: 10.1016/j.ast.2019.105466

67. Zhang J, Xiao M, Gao L, Chu S. Probability and interval hybrid reliability analysis based on adaptive local approximation of projection outlines using support vector machine. *Computer Aided Civil Infrastructure Eng.* (2019) 34:991–1009. doi: 10.1111/mice.12480

68. Fink O, Zio E, Weidmann U. Predicting component reliability and level of degradation with complex-valued neural networks. *Reliability Eng Syst Saf.* (2014) 121:198–206. doi: 10.1016/j.ress.2013.08.004

69. Brereton RG, Lloyd GR. Support vector machines for classification and regression. *Analyst.* (2010) 135:230–67. doi: 10.1039/B918972F

70. Zhang J, Xiao M, Gao L. A new method for reliability analysis of structures with mixed random and convex variables. *Appl Math Model.* (2019) 70:206–20. doi: 10.1016/j.apm.2019.01.025

71. Zhang J, Gao L, Xiao M. A new hybrid reliability-based design optimization method under random and interval uncertainties. *Int J Numer Methods Eng.* (2020) 121:4435–57. doi: 10.1002/nme.6440

72. Keshtegar B, el Amine Ben Seghier M. Modified response surface method basis harmony search to predict the burst pressure of corroded pipelines. *Eng Fail Anal.* (2018) 89:177–99. doi: 10.1016/j.engfailanal.2018.02.016

73. Keshtegar B, Heddam S. Modeling daily dissolved oxygen concentration using modified response surface method and artificial neural network: a comparative study. *Neural Comput Applic.* (2018) 30:2995–3006. doi: 10.1007/s00521-017-2917-8

74. Xiao M, Zhang J, Gao L, Lee S, Eshghi AT. An efficient Kriging-based subset simulation method for hybrid reliability analysis under random and interval variables with small failure probability. *Structural Multidiscip Optimiz.* (2019) 59:2077–92. doi: 10.1007/s00158-018-2176-z

75. Zhang J, Xiao M, Gao L, Chu S. A combined projection-outline-based active learning Kriging and adaptive importance sampling method for hybrid reliability analysis with small failure probabilities. *Comput Methods Appl Mech Eng.* (2019) 344:13–33. doi: 10.1016/j.cma.2018.10.003

76. Keshtegar B, Kisi O. Modified response-surface method: new approach for modeling pan evaporation. *J Hydrol Eng ASCE.* (2017) 22:04017045. doi: 10.1061/(ASCE)HE.1943-5584.0001541

77. Asteris PG, Nikoo M. Artificial bee colony-based neural network for the prediction of the fundamental period of infilled frame structures. *Neural Comput Appl.* (2019) 31:4837–47. doi: 10.1007/s00521-018-03965-1

78. Zhou J, Chen Y, Yong W. Performance evaluation of hybrid YYPO-RF, BWOA-RF and SMA-RF models to predict plastic zones around underground powerhouse caverns. *Geomech Geophys Geoenergy Georesources.* (2022) 8:1–29. doi: 10.1007/s40948-022-00496-x

79. Fattahi H, Hasanipanah M. An integrated approach of ANFIS-grasshopper optimization algorithm to approximate flyrock distance in mine blasting. *Eng Comput.* (2021) 38:2619–31. doi: 10.1007/s00366-020-01231-4

80. Zhou J, Guo H, Koopialipoor M, Armaghani DJ, Tahir MM. Investigating the effective parameters on the risk levels of rockburst phenomena by developing a hybrid heuristic algorithm [ESI 1%]. *Eng Comput.* (2021) 37:1679–94. doi: 10.1007/s00366-019-00908-9

81. Asteris PG, Armaghani DJ, Hatzigeorgiou Karayannis CG, Pilakoutas K. Predicting the shear strength of reinforced concrete beams using Artificial Neural Networks. *Comput Concrete.* (2019) 24:469–88. doi: 10.1016/j.engstruct.2004.01.011

82. Zhou J, Koopialipoor M, Li E, Armaghani DJ. Prediction of rockburst risk in underground projects developing a neuro-bee intelligent system. *Bull Eng Geol Environ.* (2021) 79:4265–79. doi: 10.1007/s10064-020-01788-w

83. Ye J, Koopialipoor M, Zhou J, Armaghani DJ, He X. A novel combination of tree-based modeling and Monte Carlo simulation for assessing risk levels of flyrock induced by mine blasting. *Natural Resources Res.* (2021) 30:225–43. doi: 10.1007/s11053-020-09730-3

84. Keshtegar B, Hasanipanah M, Bakhshayeshi I, Sarafraz ME. A novel nonlinear modeling for the prediction of blastinduced airblast using a modified conjugate FR method. *Measurement.* (2019) 131:35–41. doi: 10.1016/j.measurement.2018.08.052

85. Zhu SP, Keshtegar B, Chakraborty S, Trung NT. Novel probabilistic model for searching most probable point in structural reliability analysis. *Comput Methods Appl Mech Eng.* (2020) 366:113027. doi: 10.1016/j.cma.2020.113027

86. Huang J, Koopialipoor M, Armaghani DJ. A combination of fuzzy Delphi method and hybrid ANN-based systems to forecast ground vibration resulting from blasting. *Sci Rep.* (2020) 10:1–21. doi: 10.1038/s41598-020-76569-2

87. Zhou J, Li E, Wang M, Chen X, Shi X, Jiang L. Feasibility of stochastic gradient boosting approach for evaluating seismic liquefaction potential based on SPT and CPT case histories. *J Perform Constr Facil.* (2019) 33:04019024. doi: 10.1061/(ASCE)CF.1943-5509.0001292

88. Zhou J, Li C, Koopialipoor M, Jahed Armaghani D, Pham BT. Development of a new methodology for estimating the amount of PPV in surface mines based on prediction and probabilistic models (GEPMC). *Int J Min Reclam Environ.* (2020) 35:48–68. doi: 10.1080/17480930.2020.1734151

89. Yang Y, Zhang Q. A hierarchical analysis for rock engineering using artificial neural networks. *J Rock Mech Rock Eng.* (1997) 30:207–22. doi: 10.1007/BF01045717